ChemistrySelect

Research Article
doi.org/10.1002/slct.202403473

Chemistry Europe
European Chemical Societies Publishing

www.chemistryselect.org

Computational Investigation of Phytochemicals from *Aloysia citriodora* as Drug Targets for Parkinson's Disease-Associated Proteins

Yassir Boulaamane,*[a] Meriem Khedraoui,[b] Samir Chtita,[b] Iman Touati,[a] Badr-Edine Sadoq,[a] Mohammed Reda Britel,[a] and Amal Maurady[a, c]

The exact cause of Parkinson's disease is unknown, and there is currently no cure for the disease. However, there are several treatment options available to help manage its symptoms. The prevalence of PD has been increasing globally, including in Morocco. This study investigated the potential of *Aloysia citriodora*, also known as lemon verbena, for treating Parkinson's disease. Lemon verbena is a plant commonly used in Morocco for treating central nervous system related diseases. It has been traditionally used as a relaxant and sedative, and its antioxidant and antimicrobial properties have been documented. In this study, we employed molecular docking against multiple targets associated with PD to evaluate the binding affinities of the phytochemicals present in lemon verbena and elucidate their interaction profiles. Interestingly, catechin emerged as a promising bioactive molecule, outperforming reference drugs in interactions with four proteins. Pharmacokinetic/toxicity predictions were conducted to evaluate the drug-likeness of the phytocompounds. Finally, molecular dynamics simulations were performed to evaluate the stability of the protein-ligand complexes over time. By integrating computational methods, this investigation aimed to uncover the therapeutic potential of *Aloysia citriodora* compounds in Parkinson's disease management and provide valuable insights into their molecular interactions and pharmacokinetic properties. The findings of this study suggest that *Aloysia citriodora*, particularly its constituent catechin, has the potential to be a therapeutic agent for PD. Further research is needed to validate these findings in experimental and clinical settings.

1. Introduction

Parkinson's disease (PD) is a neurodegenerative disorder that affects movement.[1] It is characterized by symptoms such as tremors, stiffness, and difficulty with balance and coordination.[2] The exact cause of PD is unknown, and there is currently no cure for the disease. However, there are several treatment options available to help manage its symptoms.[3] The prevalence of Parkinson's disease has been increasing globally, including in Morocco. According to a systematic analysis of epidemiological studies, PD prevalence increased by 39.7% in Morocco between 1990 and 2016.[4] In North America, a 2022 study revealed that nearly 90000 people are diagnosed with PD each year, representing a significant increase from previous estimates.[5] The prevalence of PD in Morocco remains poorly documented. However, a study published in the Journal of Parkinson's Disease in 2020 estimated that approximately 34803 individuals were affected by the disease in 2015.[6] The management of PD typically involves a combination of medication, therapy, and in some cases, surgery.[7] Medications such as levodopa, dopamine agonists, monoamine oxidase B (MAO-B) and catechol-O-methyl transferase (COMT) inhibitors are commonly used to help control the symptoms of PD.[7] In addition to medication, physical therapy, occupational therapy, and speech therapy can also be beneficial in managing the motor symptoms of the disease. In advanced cases, deep brain stimulation surgery may be recommended to help control movement symptoms.[8] Recent research has focused on the role of alpha-synuclein and leucin-rich repeat kinase 2 (LRRK2) in PD.[9] Alpha-synuclein is a protein that forms clumps in the brains of people with PD, while LRRK2 is a gene that can contain mutations associated with an increased risk of PD.[10,11] A 2020 review article titled "Parkinson's disease: From bench to bedside" discusses the complex nature of PD, including its different etiologies and clinical features.[12] Furthermore, a review of PD research in Morocco identified studies related to the etiology and pathophysiology of PD, as well as genetic factors, which may include research on alpha-synuclein and LRRK2.[13]

Recent research has also explored other targets in PD, including dopa decarboxylase (DDC), glycogen synthase kinase 3 (GSK3), cyclooxygenase 2 (COX2), acetylcholinesterase (AChE), N-methyl-D-aspartate receptor (NMDAR), and adenosine A_{2A} receptor ($AA_{2A}R$), which are involved in neuroinflammation and

[a] *Y. Boulaamane, I. Touati, B.-E. Sadoq, M. R. Britel, A. Maurady*
Laboratory of Innovative Technologies, National School of Applied Sciences of Tangier, Abdelmalek Essaadi University, Tetouan B.P. 2117, Morocco
E-mail: y.boulaamane@gmail.com

[b] *M. Khedraoui, S. Chtita*
Laboratory of Analytical and Molecular Chemistry, Faculty of Sciences Ben M'Sik, Hassan II University of Casablanca, Casablanca B.P. 20000, Morocco

[c] *A. Maurady*
Faculty of Sciences and Techniques of Tangier, Abdelmalek Essaadi University, Tetouan B.P. 2117, Morocco

Supporting information for this article is available on the WWW under https://doi.org/10.1002/slct.202403473

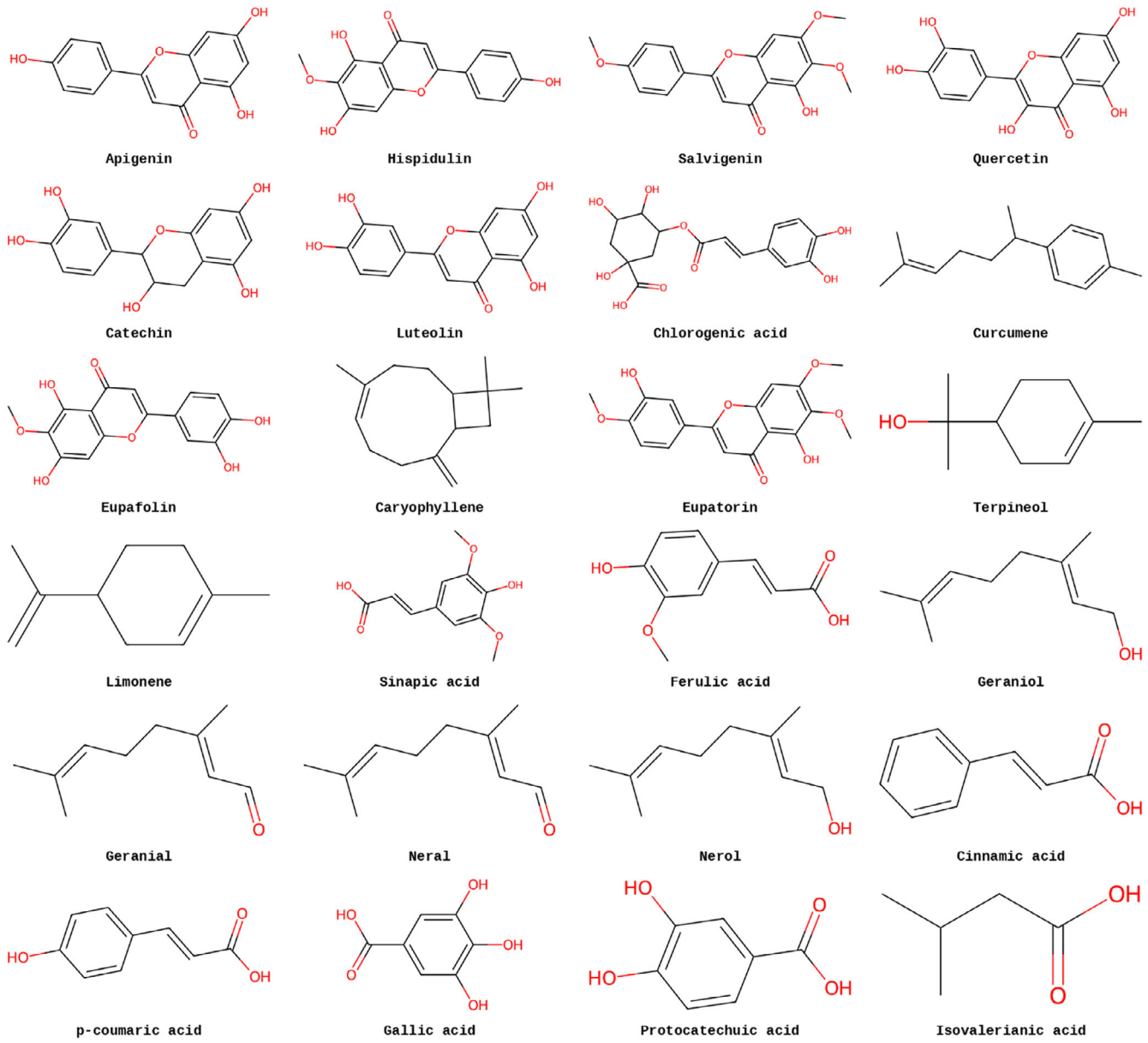

Figure 1. 2D structures of lemon verbena phytochemicals.

oxidative stress.[14,15] A 2020 review article on PD discusses the role of oxidative stress and neuroinflammation in the pathogenesis of PD and the potential of targeting these pathways for therapeutic intervention.[16] Additionally, a 2022 study on risk factors for PD in Morocco found that exposure to pesticides and heavy metals may contribute to oxidative stress and neuroinflammation, which could increase the risk of developing PD.[17]

Medicinal plants have been the focus of research for their potential therapeutic effects in PD. *Mucuna pruriens*, a plant from the Fabaceae family, has been used in Indian traditional medicine for treating PD.[18] It contains levodopa, which can help relieve PD symptoms. Additionally, *Aloysia citriodora*, also known as lemon verbena, is a plant commonly used in Morocco for treating central nervous system (CNS) related diseases, it is the most frequent medicinal plant used in brain-related diseases according to an ethnobotanical study conducted in the region of Rabat.[19] It has been traditionally used as a relaxant and sedative, and its antioxidant and antimicrobial properties have been documented.[20–22]

Following the initial exploration of medicinal plants for PD treatment, this study delves deeper into the phytochemicals present in *Aloysia citriodora*, commonly known as lemon verbena, and investigates their molecular mechanisms in treating PD. We employed molecular docking techniques against multiple targets associated with PD to elucidate the affinities and interaction profiles of these phytochemicals. Additionally, we conducted ADMET (absorption, distribution, metabolism, excretion, and toxicity) studies and molecular dynamics (MD) simulations to evaluate the stability of the protein-ligand complexes. By integrating computational methods, this investigation aims to uncover the therapeutic potential of *Aloysia citriodora*

Table 1. List of selected target proteins associated with Parkinson's disease.

Protein Name	Gene	PDB ID	Reference Drug	Ramachandran	Resolution	Reference
Adenosine A_{2A} receptor	ADORA2A	5IU4	ZM-241385	96.2% core 3.8% allowed	1.72 Å	[31]
Acetylcholinesterase	AChE	4M0E	Dihydrotanshinone I	91.4% core 8.3% allowed	2.00 Å	[32]
Alpha-synuclein	SNCA	1XQ8	Anle138b	77.4% core 13.0% allowed	NMR	[33]
Catechol-O-methyl transferase	COMT	4XUC	Q27454377	92.2% core 7.3% allowed	1.80 Å	[34]
Cyclooxygenase-2	COX2	3PGH	Flurbiprofen	80.9% core 16.4% allowed	2.50 Å	[35]
DOPA decarboxylase	DDC	1JS3	Carbidopa	91.8% core 7.5% allowed	2.25 Å	[36]
Glycogen synthase kinase 3	GSK3	1Q5K	AR-A014418	87.5% core 11.1% allowed	1.94 Å	[37]
Monoamine oxidase B	MAOB	2V5Z	Safinamide	93.5% core 5.8% allowed	1.60 Å	[38]
Ionotropic glutamate receptor	GRIN2B	5EWJ	Ifenprodil	89.3% core 10.5% allowed	2.77 Å	[39]
Metabotropic glutamate receptor	GRM1	3KS9	LY-341495	92.0% core 7.3% allowed	1.90 Å	[40]

Table 2. Grid box sizes and coordinates for each active site of the selected target proteins.

Protein Name	Gene	PDB ID	Box Size (Å)	Box Center (Å)
Adenosine A_{2A} receptor	ADORA2A	5IU4	16.5 × 21.5 × 15.0	−21.75 × 7.75 × 15.5
Acetylcholinesterase	AChE	4M0E	17.5 × 13.5 × 20.0	13.75 × −41.75 × 27.0
Alpha-synuclein	SNCA	1XQ8	18.9 × 17.2 × 20.5	−12.29 × −24.50 × −82.36
Catechol-O-methyl transferase	COMT	4XUC	14.5 × 16.0 × 17.5	−3.25 × 6.0 × −18.75
Cyclooxygenase-2	COX2	3PGH	13.0 × 19.5 × 20.0	26.0 × 18.25 × 18.0
DOPA decarboxylase	DDC	1JS3	14.0 × 15.5 × 14.5	42.5 × 37.25 × 67.25
Glycogen synthase kinase 3	GSK3	1Q5K	20.5 × 19.0 × 14.5	20.75 × 26.0 × 11.25
Monoamine oxidase B	MAOB	2V5Z	17.0 × 28.5 × 25.0	54.0 × 152.75 × 25.5
Ionotropic glutamate receptor	GRIN2B	5EWJ	26.0 × 22.0 × 23.5	84.5 × 8.5 × −31.75
Metabotropic glutamate receptor	GRM1	3KS9	25.5 × 21.5 × 24.5	−42.75 × 10.25 × 37.25

compounds in PD management and provide valuable insights into their molecular interactions and pharmacokinetic properties.

2. Materials and Methods

2.1. Data Source and Preparation of Ligands

Phytochemicals sourced from *Aloysia citriodora* were selected from Phytochemicals database (https://www.phytochemicals.info/) and based on previous literature.[23,24] PubChem database was employed to retrieve the chemical structures of the selected compounds as illustrated in Figure 1.[25] The structures of these phytochemicals were prepared by adding polar hydrogens, Gasteiger charges, and performing energy minimization using OpenBabel chemical toolbox (v3.1.1).[26] The energy minimization procedure utilized the Merck molecular force field (MMFF94) force field and included 1000 steps.[27]

2.2. Selection and Preparation of Target Proteins

The crystal structures of various proteins associated with PD were obtained from the RCSB Protein Data Bank (https://www.rcsb.org/).[28] Subsequently, the Ramachandran plots of the selected proteins were assessed using the PROCHECK tool in SAVES server (https://saves.mbi.ucla.edu/).[29] Missing residues in the selected target proteins were generated using Chimera 1.16.[30] Following the removal of unnecessary nonstandard heteroatoms, polar hydrogens were added, and Gasteiger charges were applied. All structural details of the targets were refined using the steepest descent and conjugate gradient algorithms, each comprising 100 steps, employing the Amber force field (Amber ff14SB). Subsequently, the energy-minimized protein

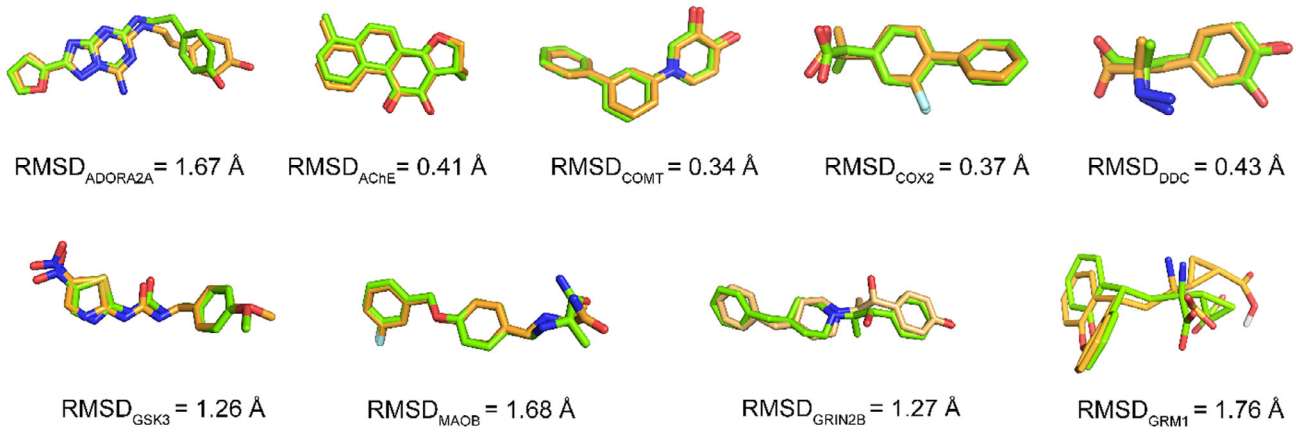

Figure 2. Accuracy of the molecular docking protocol using redocking, crystal ligands are shown in bright orange, docked ligands are shown in chartreuse.

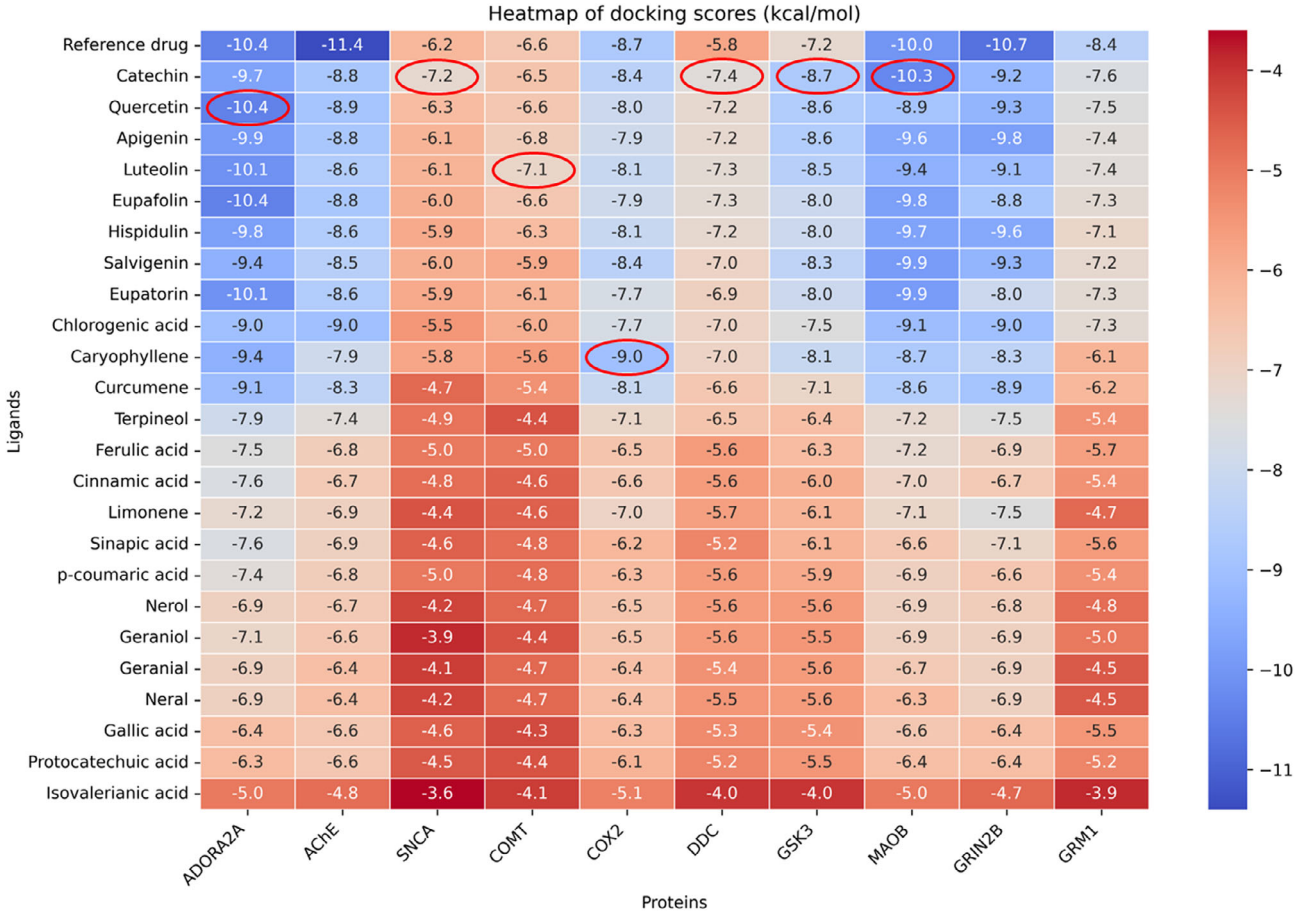

Figure 3. Molecular docking heatmap representing the binding energies (kcal/mol) of *Aloysia citriodora* chemicals with PD target proteins.

structures were converted into "pdbqt" format using the "prepare_receptor4.py" script in AutoDockTools (v1.5.6). The proteins, along with their corresponding PDB IDs are listed in Table 1.

2.3. Molecular Docking

To facilitate the molecular docking study, we developed a Python script to automate the sequential docking process using AutoDock Vina 1.1.2.[41] Grid box coordinates and dimensions in x, y, and z directions respectively were determined using the CavityPlus server (http://www.pkumdl.cn:8000/cavityplus/) with ligand mode whenever possible as shown in Table 2. Theobtained results were limited to nine binding conformations. Log files were generated, containing a list of the binding modes and their associated binding energies, which were then exported to a CSV file for ease of analysis.

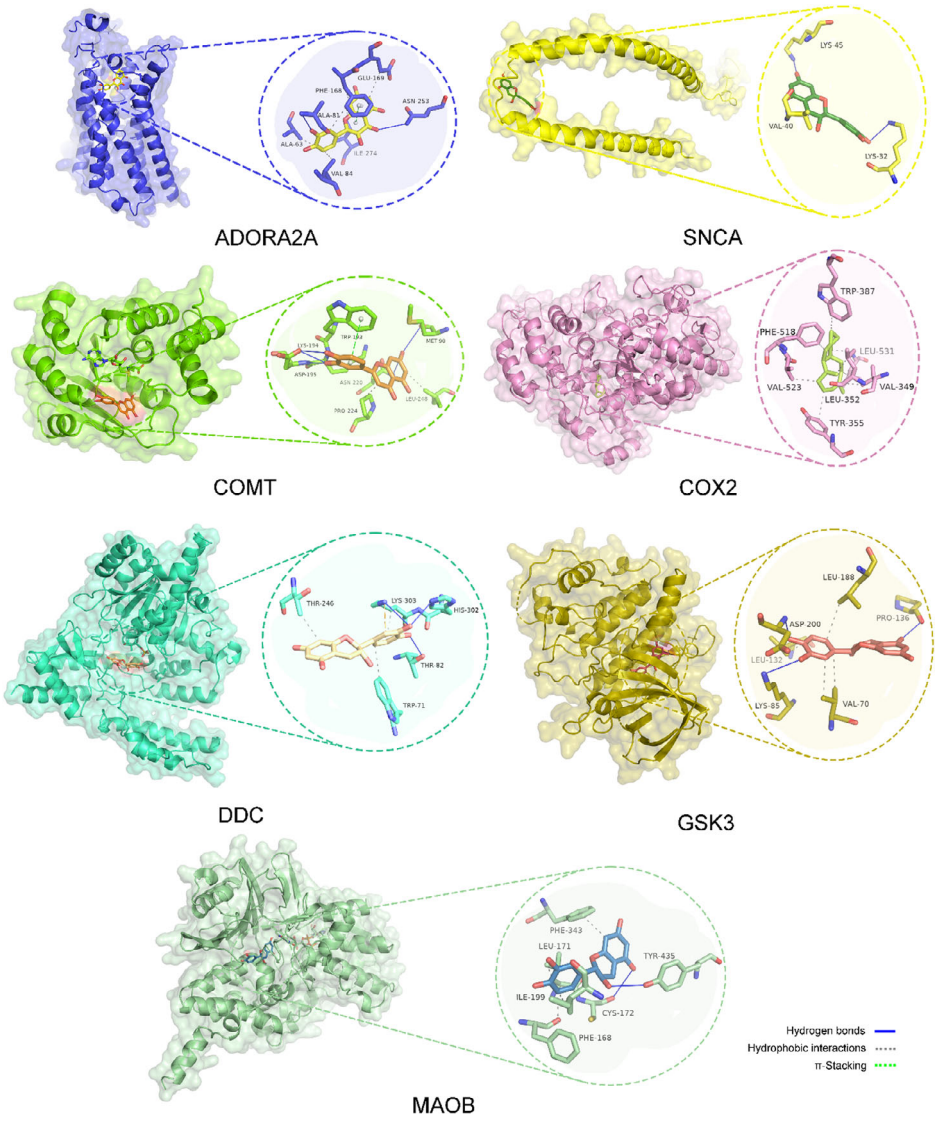

Figure 4. Molecular interactions of *Aloysia citriodora* phytochemicals with docking scores superior to those of reference drugs.

Table 3. Comparison of interaction profiles of reference drugs and selected candidates against PD-associated targets.

Protein/Ligand	Reference Drug			Best Candidate from Lemon Verbena		
	H Bonds	Hydrophobic Interactions	π-Stacking	H Bonds	Hydrophobic Interactions	π-Stacking
ADORA2A	ASN-253	LEU-85, TRP-246, LEU-249, MET-270	PHE-168	ALA-81, ASN-253	ALA-63, VAL-84, PHE-168, GLU-169, ILE-274	PHE-168
SNCA	LYS-43	TYR-39, VAL-40, LYS-43	TYR-39	VAL-40	LYS-32, VAL-40, LYS-45	–
COMT	LYS-96, LYS-194, ASN-220	TRP-88, LEU-248, ARG-251	–	MET-90, LYS-194, ASP-195, ASN-220	LYS-194, PRO-224, LEU-248	TRP-193
COX2	TYR-355	VAL-116, VAL-349, LEU-352, TYR-355, LEU-359, TYR-385, TRP-387, ALA-527, LEU-531	–	–	VAL-349, LEU-352, TYR-355, TRP-387, PHE-518, VAL-523, LEU-531	–
DDC	THR-82	TRP-71, TYR-79	–	THR-82, HIS-302, LYS-303	TRP-71, THR-246, LYS-303	–
GSK3	VAL-135, PRO-136	ILE-62	–	LYS-85, PRO-136, ASP-200	VAL-70, LEU-132, LEU-188	–
MAOB	GLN-206	LEU-171, ILE-199, ILE-316, TYR-326, PHE-343, TYR-398	–	CYS-172, TYR-435	PHE-168, LEU-171, ILE-199, PHE-343	–

Table 4. Prediction of commonly employed ADMET properties.

Compound	LogP	Water Solubility	%HIA	BBB Permeability	CYP2C9 Inhibitor	CYP3A4 inhibitior	CYP2D6 inhibitior	Total Clear-ance	AMES Toxicity	Hepato-Toxicity
ZM-241385	1.7	−3.1	75.2	−1.2	No	No	No	−0.2	No	Yes
Dihydrotanshinone I	3.3	−3.8	99.5	0.3	No	No	No	0.1	No	No
Anle138b	4.2	−3.4	92.1	0.4	No	Yes	Yes	0.1	No	Yes
1-(biphenyl-3-yl)-3-hydroxypyridin-4(1H)-one	3.2	−4.6	97.0	0.6	Yes	No	No	0.3	Yes	No
Flurbiprofen	3.7	−2.9	99.6	0.3	No	No	No	0.2	No	No
Carbidopa	−0.1	−2.5	37.2	−1.0	No	No	No	0.5	No	Yes
AR-A014418	2.4	−3.4	82.1	−0.9	No	No	No	0.0	Yes	Yes
GNE-7915	3.3	−4.1	87.4	−1.6	Yes	No	No	0.1	No	Yes
Safinamide	2.4	−2.5	94.0	−0.4	No	No	No	1.0	No	Yes
Ifenprodil	3.8	−3.4	91.2	0.4	No	No	Yes	0.7	No	Yes
Catechin	2.1	−3.1	70.4	−1.1	No	No	No	0.2	No	No
Quercetin	2.0	−2.9	77.2	−1.1	No	No	No	0.4	No	No
Luteolin	2.3	−3.1	81.1	−0.9	Yes	No	No	0.5	No	No
Apigenin	2.6	−3.3	93.3	−0.7	No	No	No	0.6	No	No
Eupafolin	2.3	−3.2	77.3	−1.4	No	No	No	0.5	No	No
Hispidulin	2.6	−3.4	84.7	−1.1	Yes	No	No	0.5	No	No
Salvigenin	3.2	−3.9	95.9	−0.7	No	Yes	No	0.7	No	No
Eupatorin	2.9	−3.3	99.5	−0.7	No	Yes	No	0.6	No	No
Caryophyllene	4.7	−5.6	94.8	0.7	No	No	No	1.1	No	No
Chlorogenic acid	−0.6	−2.4	36.4	−1.4	No	No	No	0.3	No	No
Curcumene	4.8	−6.0	93.3	0.6	No	No	No	1.5	No	No
Terpineol	2.5	−2.0	94.2	0.3	No	No	No	1.2	No	No
Ferulic acid	1.5	−2.8	93.7	−0.2	No	No	No	0.6	No	No
Limonene	3.3	−3.6	95.9	0.7	No	No	No	0.2	No	No
Cinnamic acid	1.8	−2.6	94.8	0.4	No	No	No	0.8	No	No
Sinapic acid	1.5	−2.9	93.1	−0.2	No	No	No	0.7	No	No
p-coumaric acid	1.5	−2.4	93.5	−0.2	No	No	No	0.7	No	No
Nerol	2.7	−2.9	92.8	0.6	No	No	No	0.4	No	No
Geraniol	2.7	−2.9	92.8	0.6	No	No	No	0.4	No	No
Geranial	2.9	−3.4	95.3	0.6	No	No	No	0.4	No	No
Neral	2.9	−3.4	95.3	0.6	No	No	No	0.4	No	No
Gallic acid	0.5	−2.6	43.4	−1.1	No	No	No	0.5	No	No
Protocatechuic acid	0.8	−2.1	71.2	−0.7	No	No	No	0.6	No	No
Isovalerianic acid	1.1	−0.8	88.8	−0.2	No	No	No	0.4	No	No

2.4. ADMET Study

To understand how our candidate ligands interact with the body, we investigated their pharmacokinetic and toxicity properties. These properties are determined by the inherent physicochemical characteristics and molecular fingerprints of each ligand. These characteristics influence how the ligands interact with transport proteins and enzymes that affect drug clearance. In this study, we utilized pkCSM, a web server, to predict key ADMET parameters for our ligands.[42] These parameters include water solubility, blood-brain barrier (BBB) permeability, cytochrome P450 inhibition, total clearance, and potential Ames and liver toxicity. This comprehensive ADMET analysis allowed us to make informed decisions about the suitability of our candidate ligands.

2.5. Molecular Dynamics Simulations and Free Energy Calculations

To verify the reliability of molecular docking, molecular dynamics (MD) simulations were conducted on the complexes from the best configuration obtained after docking, using GROMACS software (v2023).[43] The Optimized Potentials for Liquid

Simulations-All Atom (OPLS-AA) force field was employed for the protein, and the ligand topology was generated using the SwissParam server.[44] All complexes were solvated using TIP3P water molecules in a dodecahedron box maintaining a distance of 1 nm from the center of the protein, and the net charges of the systems were neutralized by adding salt at a concentration of 0.15 M. Energy minimization was performed using the steepest descent integrator to achieve minimum energy and maximum force. The system was equilibrated for 1 ns under "isothermal-isobaric" (NVT) and (NPT) conditions, using the Berendsen thermostat and the Parinello-Rahman barostat. The Berendsen thermostat and Parinello-Rahman barostat were used to maintain temperature and pressure.[45,46] Subsequently, MD production runs were executed for 100 ns for each of the seven complexes. Output trajectories were generated, and files were evaluated to better understand the behavior of the studied complexes.[47]

3. Results and Discussion

3.1. Molecular Docking Protocol Validation

In our docking protocol validation, we employed a rigorous process using redocking and superimposition to ensure accuracy and reliability, as supported by recent studies.[48–50] The root-mean-square deviation (RMSD) was used to assess how closely the docked pose matched the reference structure, with values below 2.0 Å considered acceptable for reliable docking. Lower RMSD values indicate higher precision in ligand placement within the target protein.

To validate the accuracy of AutoDock Vina, we performed redocking by downloading the co-crystallized ligands of each target protein from PubChem and redocking them into their active sites. Figure 2 shows the RMSD between the reference native ligands and docked ligands. Correct conformations (RMSD < 2 Å) were predicted for all the ligands.

3.2. Molecular Docking Results

In this investigation, we conducted docking simulations of 24 compounds sourced from *Aloysia citriodora* against 10 target proteins associated with PD.

Figure 3 illustrates a heatmap depicting the binding energies estimated from the docking poses of *Aloysia citriodora* compounds across the evaluated molecular targets of PD. The heatmap's color scale, ranging from red (indicating the lowest binding affinity) to blue (indicating the highest), was determined based on the docking outcomes. Within the heatmap, circles highlight the binding interactions of ligands with lower binding energies than the native ligands of PD target proteins. Notably, compounds such as catechin, quercetin, luteolin, and apigenin exhibited substantial binding affinity with most of the selected PD-related proteins. Specifically, catechin demonstrated superior binding affinity compared to reference drugs across four of the ten tested PD proteins. Additionally, other compounds such as quercetin, luteolin, and caryophyllene achieved higher scores than the reference drugs targeting $AA_{2A}R$, COMT, and COX2.

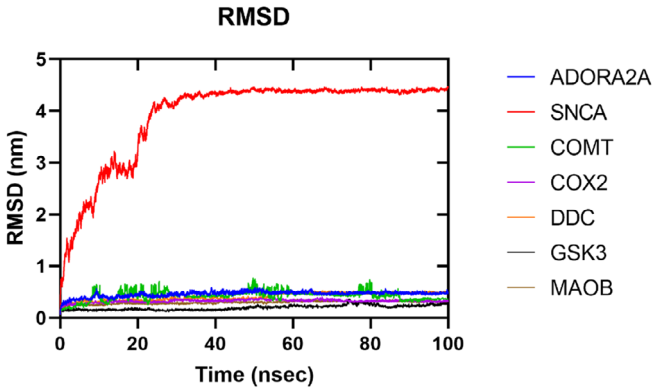

Figure 5. Root-mean square deviation (RMSD) of the selected protein-ligand complexes throughout the 100 ns simulation time.

Figure 4 illustrates the binding conformations of *Aloysia citriodora* phytochemicals, which exhibited superior affinity compared to reference drugs in molecular docking studies against seven of the ten target proteins. The phytochemicals achieved significantly higher docking scores than the reference drugs. Detailed visualizations of the binding modes—such as catechin bound to SNCA, DDC, GSK3, and MAOB, quercetin-ADORA2A, luteolin-COMT, and caryophyllene-COX2—were generated using Ligplot$^+$ (version 2.2)[51] and are shown in Figures S1–S7 of the Supplementary Information.

The lemon verbena phytochemicals demonstrate intriguing potential as therapeutic agents when compared to reference drugs. In some cases, like with $AA_{2A}R$ (ADORA2A), they closely mimic the reference drug's interactions as shown in Table 2. For proteins like ASYN and COMT, the lemon verbena compounds show a similar binding location to the reference drug but form additional or stronger interactions, suggesting enhanced binding abilities. Interestingly, with targets like COMT, DDC, GSK3, and MAOB, the phytochemicals exhibit distinct interaction profiles, indicating the involvement of other critical amino acids in ligand binding such as CYS-172 in MAOB which has been demonstrated to play a role in anchoring and stabilizing ligands within the aromatic cage of the substrate cavity.[52] These results highlight the need for further experimental validation to determine the true potential of lemon verbena phytochemicals in targeting these specific proteins for therapeutic purposes.

3.3. ADMET Prediction

Table 3 highlights key differences in ADMET properties between the reference drugs and promising phytochemicals: catechin, quercetin, luteolin, and caryophyllene. The reference drugs exhibit a wider range of ADMET profiles. The flavonoids (catechin, quercetin, and luteolin) show similar predicted water solubility to some reference drugs, but with potentially lower intestinal absorption. This might necessitate specific formulation strategies to improve bioavailability.[53] However, despite their low predicted BBB permeability scores suggesting a limited

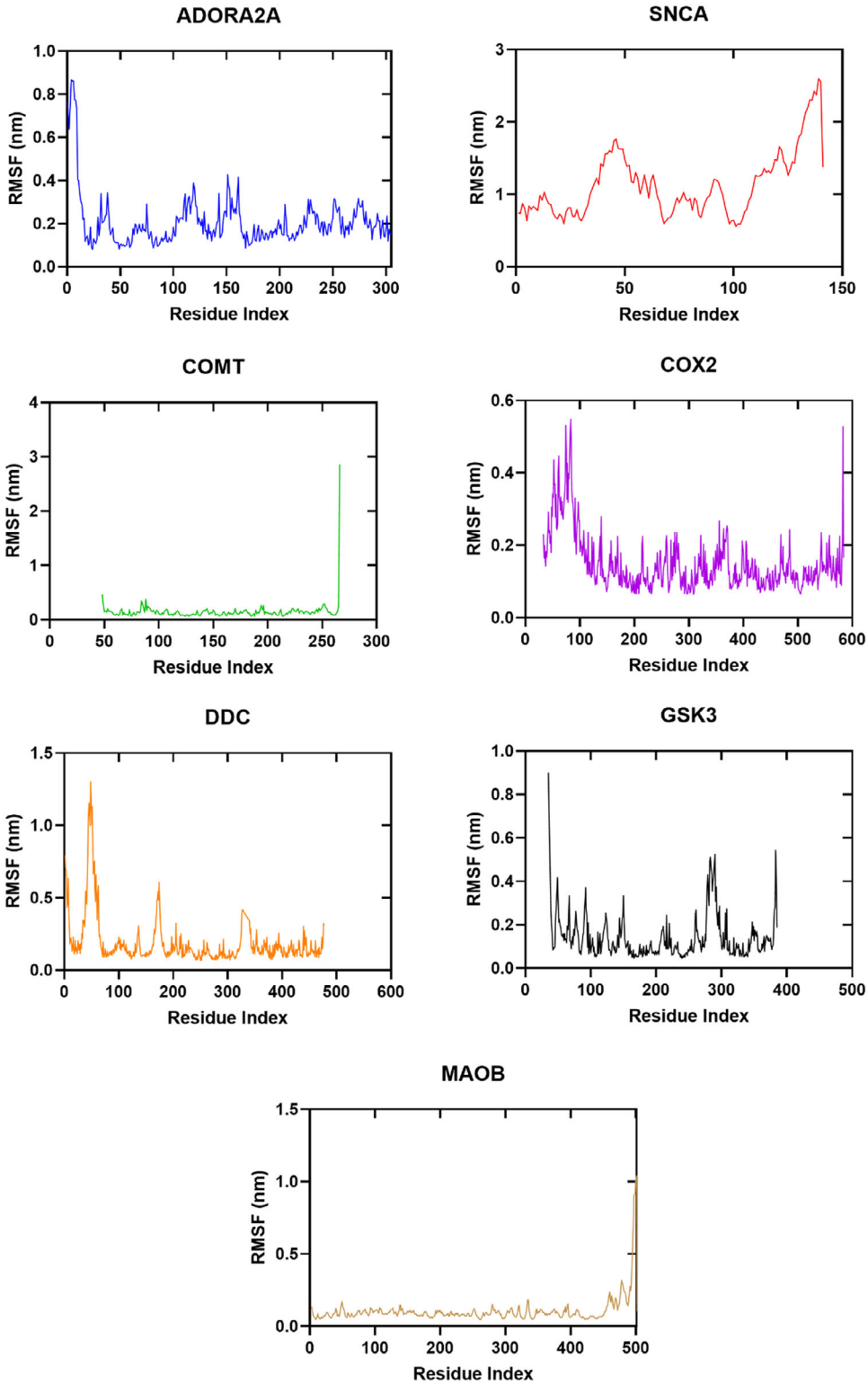

Figure 6. Root-mean square fluctuation (RMSF) of the studied protein-ligand complexes capturing average fluctuations per residue.

ability to target the central nervous system (CNS), experimental studies report measurable BBB permeability for flavonoids. These studies indicate that lipophilicity and interactions with efflux transporters can significantly influence brain penetration.[54,55] The moderate lipophilicity (LogP $\leq$ 3) of these flavonoids further supports their potential for some level of brain penetration. To improve the predicted limited BBB permeability of these compounds, several strategies could be explored in future studies. One option is to modify the chemical structure to increase lipophilicity, thereby enhancing their ability to cross the BBB.

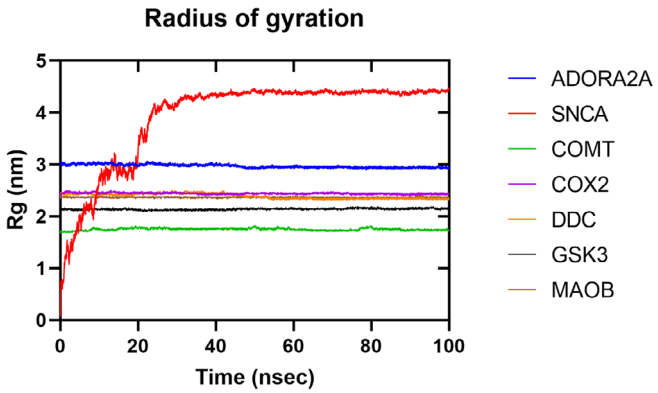

Figure 7. Radius of gyration measuring the compactness of each protein-ligand complex throughout the 100 ns simulation time.

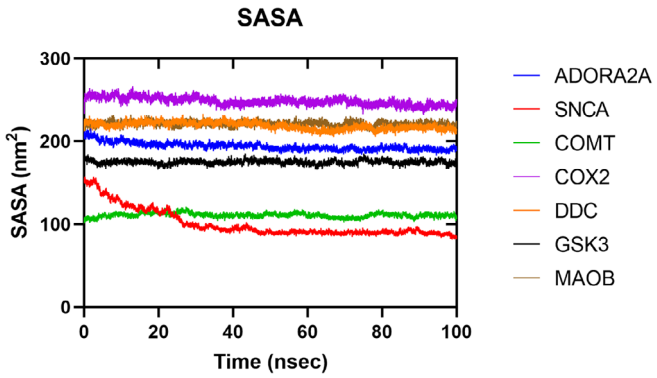

Figure 8. Solvent accessible surface area (SASA) quantifying the surface area of the protein ligand complexes that is exposed to the solvent throughout the 100 ns simulation time.

Another approach is to employ prodrug strategies, where inactive derivatives are designed to pass through the BBB and then convert to active forms within the CNS. Nanotechnology-based delivery systems, such as nanoparticles or liposomes, offer another promising solution, as they can be engineered to facilitate transport across the BBB. Additionally, targeting specific transport mechanisms, like receptor- or carrier-mediated transcytosis, could enhance brain penetration. These strategies will be essential in future efforts to optimize CNS delivery. Cytochrome P450 inhibition was predicted to assess the potential for drug-drug interactions (DDIs), focusing on CYP2C9, CYP3A4, and CYP2D6, which are critical for CNS drug metabolism. Several reference drugs showed a higher risk of CYP2C9 inhibition, while the flavonoids (catechin, quercetin, luteolin) presented a lower risk, potentially minimizing DDIs. Most phytochemicals did not inhibit CYP3A4, but salvigenin and eupatorin did, raising concerns about interactions with PD medications metabolized by this enzyme. For CYP2D6, anle138b and ifenprodil were inhibitors, while catechin, quercetin, and luteolin were not, suggesting a lower risk of DDIs with drugs metabolized by CYP2D6.

Caryophyllene, on the other hand, presents a unique profile with very low water solubility and high clearance. Interestingly, it also exhibits surprisingly good predicted BBB permeability as shown in Table 4.[56] If formulation challenges can be addressed to enhance bioavailability, caryophyllene's potential CNS access opens doors for neurological applications. To address the issue of low water solubility, various formulation strategies could be considered to improve caryophyllene's bioavailability. Techniques such as nanoparticle-based delivery systems, solid lipid nanoparticles (SLNs), or liposomal formulations may enhance solubility and facilitate absorption.[57,58] Additionally, sublingual formulations present an attractive option as they bypass the gastrointestinal tract, avoiding first-pass metabolism and potentially improving bioavailability.[59,60] Other approaches, including cyclodextrin complexation or nanoemulsions, could further stabilize caryophyllene in biological systems, making these strategies crucial for translating its therapeutic potential in PD.[59,60]

3.4. Molecular Dynamics Analysis

MD simulations were performed to evaluate the stability and dynamic behavior of the protein-ligand complexes over a 100 ns timeframe. MD simulations allow us to investigate how the complexes evolve in a simulated physiological environment, offering insights into the stability of the protein structures and their interactions with ligands.[61,62] Key parameters such as the root-mean-square deviation (RMSD), root-mean-square fluctuation (RMSF), radius of gyration (Rg), solvent-accessible surface area (SASA), and hydrogen bond formation were calculated to assess the stability and compactness of each complex. These analyses provide critical information on the ligand-binding strength and overall stability, guiding the potential of these complexes for therapeutic application.

3.4.1. Root-Mean Square Deviation

According to the RMSD trajectories, it can be observed that the complexes: COMT, COX2, GSK3, and MAOB were stabilized at approximately 0.20 nm, while ADORA2A and DDC reached around 0.30 nm. The alpha-synuclein monomer (SNCA), on the other hand, initially showed a significant rise in RMSD, reaching as high as 4.5 nm within the first 25 ns, suggesting a conformational change during this early phase of the simulation. However, after this point, SNCA remained stable for the rest of the simulation, indicating that its structure stabilized after the initial fluctuations, consistent with previous findings.[63–65] Based on Figure 1, many RMSD curves appear to fluctuate slightly, indicating the stability of the protein structures and the ligand binding strength in the active site pockets. As long as the complexes exhibit comparable RMSD trajectories with very little deviation throughout the simulation process, this indicates that they have more potential success in terms of stability and ligand binding. The SNCA complex, while demonstrating stability after the initial conformational change, may require further investigation to understand the implications of this early instability (Figure 5).

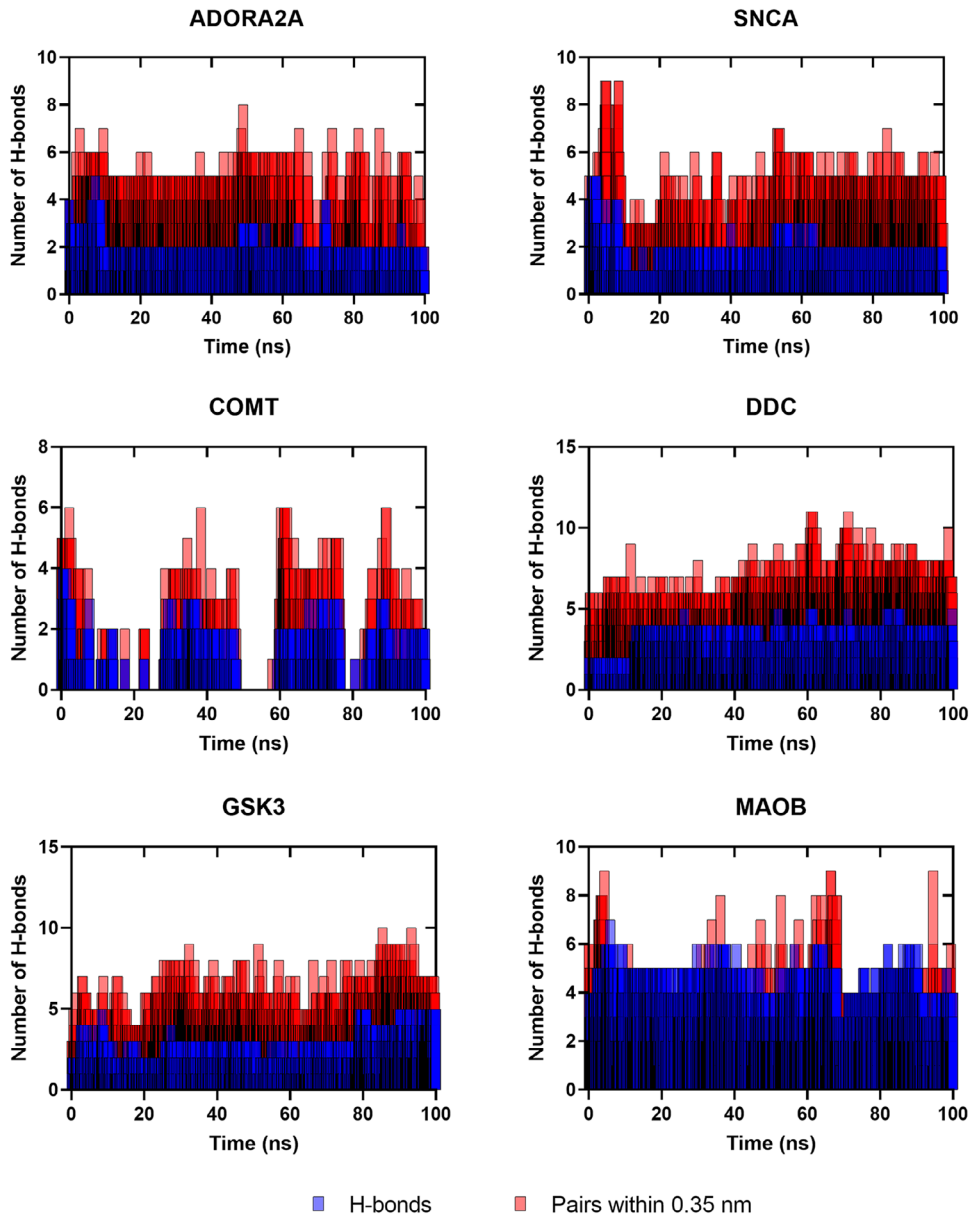

Figure 9. Hydrogen bonds and number of pairs within 0.35 nm formed during 100 ns MD simulations.

3.4.2. Root-Mean Square Fluctuation

The RMSF measurement shows us the contribution of individual protein residues to the structural fluctuations of the complex. The complexes 3GPH, ADORA2A, COMT, DDC, GSK3, and MAOB were located within the RMSF range of 0.1 to 0.5 nm over the 100 ns simulation period, while the average RMSF value for SNCA is 1.5 nm (Figure 2). We observe that the RMSF of these proteins in the complexes 3GPH, ADORA2A, COMT, DDC, GSK3, and MAOB did not deviate much, and the average RMSF values remained constant, suggesting that they were not disrupted during ligand binding. The RMSF results of the residues were considered to have reduced mobility and low fluctuations, indicating that these complexes have a low tendency to destabilize. As for the SNCA-catechin complex, it underwent significant fluctuations with higher RMSF values than the other complexes, which is consistent with the elevated results of their RMSD trajectory. Overall, the RMSF results reinforce the idea that the majority of these protein-ligand complexes maintained their stability, while the SNCA-catechin complex requires further exploration due to its higher degree of fluctuation (Figure 6).

3.4.3. Radius of Gyration

The radius of gyration (Rg) analysis revealed that all protein complexes maintained their structural stability throughout the 100 ns MD simulation, indicating minimal structural fluctuations. Rg values remained relatively constant, with ADORA2A, SNCA, COMT, COX2, DDC, GSK3, and MAOB exhibiting values of 3.00 nm, 4.20 nm, 1.65 nm, 2.10 nm, 2.33 nm, 2.08 nm, and 2.37 nm, respectively. While the Rg value for SNCA is slightly higher compared to the other complexes, It exhibits minimal fluctuations after 25

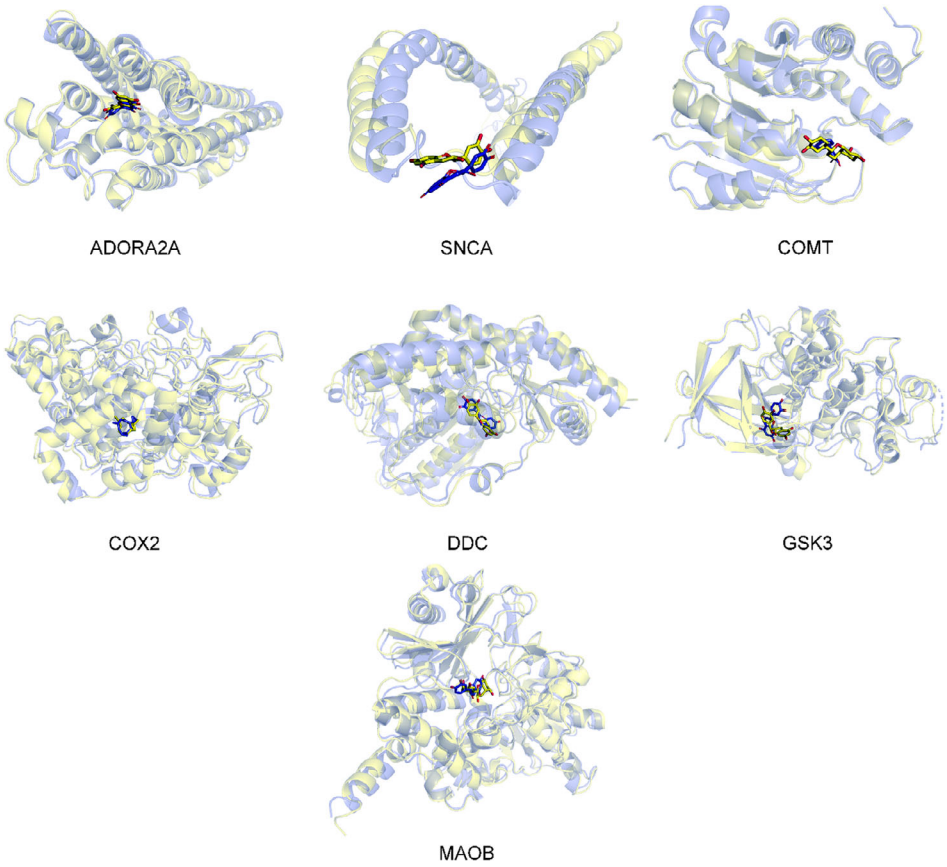

Figure 10. Conformation snapshots of the studied complexes at 0 ns (yellow) and 100 ns (blue) after recentring and rewrapping coordinates.

ns, suggesting good stability and structural integrity.[63] Overall, the consistent Rg values suggest that all complexes are stable and maintain their structural integrity, supporting the validity of the models used and the reliability of the results obtained (Figure 7).[66]

3.4.4. Solvent-Accessible Surface Area

The SASA analysis revealed that all protein-ligand complexes maintained their structural stability throughout the 100 ns MD simulation, indicating minimal fluctuations in the molecular surface exposed to solvent. SASA values remained relatively constant, with ADORA2A, SNCA, COMT, COX2, DDC, GSK3, and MAOB exhibiting values of 300 nm^2, 195 nm^2, 104 nm^2, 250 nm^2, 189 nm^2, 226 nm^2, and 97 nm^2, respectively. While some complexes, like SNCA and ADORA2A, showed slight fluctuations in SASA during the early stages of the simulation, these fluctuations were minimal and did not compromise the overall stability of the complexes.[67] The consistent SASA values suggest that the protein-ligand complexes are compact and resistant to denaturation, highlighting their stability and functional relevance (Figure 8).[68]

3.4.5. Hydrogen Bonds

To further deepen the understanding of the previous results, we also investigated the formation of hydrogen bonds through MD simulations, as it is important to consider the properties of hydrogen bonds in drug design due to their strong influence on drug specificity.[69] As shown in Figure 9, the complexes ADORA2A, COMT, DDC, GSK3, MAOB, and SNCA averaged three, five, three, four, five, and two hydrogen bonds, respectively. Consequently, the ligands remained close to the protein binding site due to the establishment of hydrogen bonds, which promote the formation of a stable complex. Regarding the caryophyllene-COX2 complex, no hydrogen bonds were observed throughout the 100 ns molecular dynamics simulation. This is consistent with the molecular structure of caryophyllene, which lacks hydrogen bond donors or acceptors. Therefore, the interactions between caryophyllene and COX2 are predominantly hydrophobic in nature, as predicted by the molecular docking analysis. This lack of hydrogen bonding also suggests that the binding affinity of caryophyllene to COX2 is primarily driven by van der Waals forces and hydrophobic interactions, which may contribute to the compound's overall stability within the binding pocket.

Figure 10 illustrates the conformational stability of the studied protein-ligand complexes over a 100 ns MD simulation. The complexes were initially prepared at 0 ns (depicted in yellow) and their final conformations at 100 ns (depicted in blue) were obtained after re-centering and re-wrapping the coordinates to account for any potential drift or periodic boundary effects during the simulation. The high degree of overlap between the initial and final conformations of the protein backbone (blue and yellow) suggests that the overall structure of the proteins

remained relatively stable throughout the simulation. Minor deviations can be attributed to the inherent flexibility of the protein structure and the dynamic nature of the interactions with the ligands.

4. Conclusion

This study explored the potential of *Aloysia citriodora* phytochemicals as therapeutic agents for Parkinson's disease through a multi-faceted computational approach. Molecular docking revealed promising binding affinities for several compounds, particularly catechin, across multiple PD-related targets. Notably, catechin outperformed reference drugs in interactions with four proteins (SNCA, DDC, GSK3, and MAOB), while still exhibiting promising affinities toward ADORA2A, COX2, and GRIN2B, suggesting its potential as a lead compound. Furthermore, catechin's favorable pharmacokinetic properties, including lower risk of CYP-mediated drug-drug interactions and predicted blood-brain barrier permeability, highlight its potential clinical relevance. While standard PD treatments such as levodopa and dopamine agonists primarily target symptom management, catechin may offer broader therapeutic benefits by interacting with multiple PD targets, potentially addressing both motor and non-motor symptoms through its multi-target profile. While *Aloysia citriodora* demonstrates promise for PD treatment, further investigation is required. Experimental validation is crucial to confirm the observed interactions and assess the biological activity of these phytochemicals in relevant models. Additionally, formulation strategies should be explored to address bioavailability challenges, particularly for compounds like caryophyllene with low water solubility. The unique ADMET profiles of different phytochemicals, such as catechin's potential for peripheral effects and caryophyllene's potential for CNS penetration, should be considered in future drug development efforts.

Acknowledgements

The authors have nothing to report.

Conflict of Interests

The authors declare no conflict of interest.

Data Availability Statement

The data that support the findings of this study are available from the corresponding author upon reasonable request.

Keywords: ADMET prediction · *Aloysia citriodora* · Molecular docking · Molecular dynamics simulations · Parkinson's disease

[1] D. K. Simon, C. M. Tanner, P. Brundin, *Clin. Geriatr. Med.* **2020**, *36*, 1–12.
[2] M. J. Armstrong, M. S. Okun, *J. Am. Med. Assoc.* **2020**, *323*, 548–560.
[3] K. R. Chaudhuri, M. A. Qamar, T. Rajah, P. Loehrer, A. Sauerbier, P. Odin, P. Jenner, *NPJ Parkinsons Dis.* **2016**, *2*, 1–7.
[4] A. Achbani, A. Ougjij, S. A. Wahmane, H. Sine, A. Kharbach, Y. Bouchriti, A. Belmouden, M. Nejmeddine, *Arc. Neurosci.* **2022**, *9*, 126351.
[5] A. W. Willis, E. Roberts, J. C. Beck, B. Fiske, W. Ross, R. Savica, S. K. Van Den Eeden, C. M. Tanner, C. Marras, *Parkinson's Dis.* **2022**, *8*, 1–71.
[6] H. Khalil, L. M. Chahine, J. Siddiqui, M. Salari, S. El-Jaafary, Z. Aldaajani, M. Abu Al-Melh, T. M. Mohammad, M. A. Snineh, N. A. Syed, M. Bhatt, *J. Parkinsons Dis.* **2020**, *10*, 729–741.
[7] B. S. Connolly, A. E. Lang, *J. Am. Med. Assoc.* **2014**, *311*, 1670–1683.
[8] M. Kogan, M. McGuire, J. Riley, Deep Brain Stimulation for Parkinson Disease. Neurosurgery Clinics of North America, **2019**, *30*, 137–146, https://doi.org/10.1016/j.nec.2019.01.001.
[9] L. V. Kalia, S. K. Kalia, A. E. Lang, *Movement Disorders* **2015**, *30*, 1442–1450.
[10] I. Fujiwara, S. Takahashi, H. Tadakuma, T. Funatsu, S. I. Ishiwata, *Nat. Cell Biol.* **2002**, *4*, no. pp. 160–164.
[11] J. Q. Li, L. Tan, J. T. Yu, *Mol. Neurodegener.* **2014**, *9*, 47.
[12] A. Draoui, O. El Hiba, A. Aimrane, A. El Khiat, H. Gamrani, *Rev. Neurol.* **2020**, *176*, 543–559.
[13] M. Daghi, A. Lakhdar, H. El Otmani, *Neurodegener. Dis. Manag.* **2023**, *13*, 129–139.
[14] R. Gordon, T. M. Woodruff, Chapter 3 Neuroinflammation as a therapeutic target in neurodegenerative diseases, In V. Baekelandt & E. Lobbestael (Eds.), *Disease-Modifying Targets in Neurodegenerative Disorders*, Academic Press **2017** pp. 49–80, https://doi.org/10.1016/B978-0-12-805120-7.00003-8.
[15] A. Y. Sun, Y.-M. Chen, *J. Biomed. Sci.* **1998**, *5*, 401–414.
[16] O. Hwang, *Exp. Neurobiol.* **2013**, *22*, 11.
[17] A. Achbani, A. Ougjij, S. A. Wahmane, H. Sine, A. Kharbach, Y. Bouchriti, A. Belmouden, M. Nejmeddine, *Arch. Neurosci.* **2022**, *9*, 126351.
[18] S. N. Rai, V. K. Chaturvedi, P. Singh, B. K. Singh, M. P. Singh, *3 Biotech.* **2020**, *10*, 1–11.
[19] S. Hseini, A. Kahouadji, *Lazaroa* **2007**, *28*, 84.
[20] M. Sabti, K. Sasaki, C. Gadhi, H. Isoda, *Int. J. Mol. Sci.* **2019**, *20*, 3556, https://doi.org/10.3390/IJMS20143556.
[21] H. M. Rashid, A. I. Mahmod, F. U. Afifi, W. H. Talib, *Plants* **2022**, *11*, 785.
[22] M. R. Kachmar, H. N. Mrabti, M. Bellahmar, A. Ouahbi, Z. Haloui, K. El Badaoui, A. Bouyahya, S. Chakir, *Evid. Based Complement Alternat. Med.* **2021**, *2021*, 20, https://doi.org/10.1155/2021/6002949.
[23] R. Bahramsoltani, P. Rostamiasrabadi, Z. Shahpiri, A. M. Marques, R. Rahimi, M. H. Farzaei, *J. Ethnopharmacol.* **2018**, *222*, 34–51.
[24] A. Hematian Sourki, A. Ghani, F. Kiani, A. Alipour, *Food Sci. Nutr.* **2021**, *9*, 3100.
[25] S. Kim, J. Chen, T. Cheng, A. Gindulyte, J. He, S. He, Q. Li, B. A. Shoemaker, P. A. Thiessen, B. Yu, L. Zaslavsky, *Nucleic Acids Res.* **2019**, *47*, D1102–D1109.
[26] N. M. O'Boyle, M. Banck, C. A. James, C. Morley, T. Vandermeersch, G. R. Hutchison, *J Cheminform.* **2011**, *3*, 1–14.
[27] J. B. Hendrickson, *J. Am. Chem. Soc.* **1961**, *83*, 4537–4547.
[28] A. Kouranov, L. Xie, J. de la Cruz, L. Chen, J. Westbrook, P. E. Bourne, H. M. Berman, *Nucleic Acids Res.* **2006**, *34*, D302–D305.
[29] R. A. Laskowski, M. W. MacArthur, D. S. Moss, J. M. Thornton, *J. Appl. Crystallogr.* **1993**, *26*, 283–291.
[30] E. F. Pettersen, T. D. Goddard, C. C. Huang, G. S. Couch, D. M. Greenblatt, E. C. Meng, T. E. Ferrin, *J. Comput. Chem.* **2004**, *25*, 1605–1612, https://doi.org/10.1002/jcc.20084.
[31] E. Segala, D. Guo, R. K. Cheng, A. Bortolato, F. Deflorian, A. S. Doré, J. C. Errey, L. H. Heitman, A. P. IJzerman, F. H. Marshall, R. M. Cooke, *J. Med. Chem.* **2016**, *59*, 6470–6479.
[32] J. Cheung, E. N. Gary, K. Shiomi, T. L. Rosenberry, *ACS Med. Chem. Lett.* **2013**, *4*, 1091–1096.
[33] T. S. Ulmer, A. Bax, N. B. Cole, R. L. Nussbaum, *J. Biol. Chem.* **2005**, *280*, 9595–9603.
[34] S. T. Harrison, M. S. Poslusney, J. J. Mulhearn, Z. Zhao, N. R. Kett, J. W. Schubert, J. Y. Melamed, T. J. Allison, S. B. Patel, J. M. Sanders, S. Sharma, *ACS Med. Chem. Lett.* **2015**, *6*, 318–323.
[35] R. G. Kurumbail, A. M. Stevens, J. K. Gierse, J. J. McDonald, R. A. Stegeman, J. Y. Pak, D. Gildehaus, J. M. Iyashiro, T. D. Penning, K. Seibert, P. C. Isakson, *Nature* **1996**, *384*, 644–648.

[36] P. Burkhard, P. Dominici, C. Borri-Voltattorni, J. N. Jansonius, V. N. Malashkevich, *Nature Struc. Biol.* **2001**, *8*, 963–967.
[37] R. Bhat, Y. Xue, S. Berg, S. Hellberg, M. Ormö, Y. Nilsson, A. C. Radesäter, E. Jerning, P. O. Markgren, T. Borgegård, M. Nylöf, *J. Biol. Chem.* **2003**, *278*, 45937–45945.
[38] C. Binda, J. Wang, L. Pisani, C. Caccia, A. Carotti, P. Salvati, D. E. Edmondson, A. Mattevi, *J. Med. Chem.* **2007**, *50*, 5848–5852.
[39] D. Stroebel, D. L. Buhl, J. D. Knafels, P. K. Chanda, M. Green, S. Sciabola, L. Mony, P. Paoletti, J. Pandit, *Mol. Pharmacol.* **2016**, *89*, 541–551.
[40] A. B. Seven, X. Barros-Álvarez, M. de Lapeyrière, M. M. Papasergi-Scott, M. J. Robertson, C. Zhang, R. M. Nwokonko, Y. Gao, J. G. Meyerowitz, J. P. Rocher, D. Schelshorn, *Nature* **2021**, *595*, 450–454.
[41] O. Trott, A. J. Olson, *J. Comput. Chem.* **2010**, *31*, 455–461.
[42] D. E. V. Pires, T. L. Blundell, D. B. Ascher, *J. Med. Chem.* **2015**, *58*, 4066–4072.
[43] M. J. Abraham, T. Murtola, R. Schulz, S. Páll, J. C. Smith, B. Hess, E. Lindahl, *SoftwareX* **2015**, *1–2*, 19–25, https://doi.org/10.1016/j.softx.2015.06.001.
[44] V. Zoete, M. A. Cuendet, A. Grosdidier, O. Michielin, *J. Comput. Chem.* **2011**, *32*, 2359–2368, https://doi.org/10.1002/jcc.21816.
[45] G. Bussi, D. Donadio, M. Parrinello, *J. Chem. Phys.* **2007**, *126*, 014101, https://doi.org/10.1063/1.2408420.
[46] M. Parrinello, A. Rahman, *J. Appl. Phys.* **1981**, *52*, 7182–7190, https://doi.org/10.1063/1.328693.
[47] Y. Boulaamane, P. Kandpal, A. Chandra, M. R. Britel, A. Maurady, *J. Biomol. Struct. Dyn.* **2023**, *42*, 1629–1646, https://doi.org/10.1080/07391102.2023.2209650.
[48] M. Shah, R. Yamin, I. Ahmad, G. Wu, Z. Jahangir, A. Shamim, H. Nawaz, U. Nishan, R. Ullah, E. A. Ali Sheheryar, *PLoS One* **2024**, *19*, e0294769, https://doi.org/10.1371/JOURNAL.PONE.0294769.
[49] R. Yamin, I. Ahmad, H. Khalid, A. Perveen, S. W. Abbasi, U. Nishan, S. Sheheryar, A. A. Moura, S. Ahmed, R. Ullah, E. A. A, *Front. Pharmacol.* **2024**, *15*, 1369659.
[50] I. Ahmad, H. Khalid, A. Perveen, M. Shehroz, U. Nishan, F. U. Rahman Sheheryar, A. A. Moura, R. Ullah, E. A. Ali, M. Shah, *ACS Omega* **2024**, *9*, 16262–16278.
[51] R. A. Laskowski, M. B. Swindells, *J. Chem. Inf. Model.* **2011**, *51*, 2778–2786.
[52] A. Irfan, A. F. Zahoor, Y. Boulaamane, S. Javed, H. Hameed, A. Maurady, M. T. Muhammed, S. Ahmad, A. A. Al-Mutairi, I. Shahzadi, S. A. Al-Hussain, *Front. Chem.* **2024**, *12*, 1449165.
[53] A. Faria, D. Pestana, D. Teixeira, P. O. Couraud, I. Romero, B. Weksler, V. de Freitas, N. Mateus, C. Calhau, *Food Funct.* **2011**, *2*, 39–44.
[54] K. A. Youdim, M. S. Dobbie, G. Kuhnle, A. R. Proteggente, N. J. Abbott, C. Rice-Evans, *J. Neurochem.* **2003**, *85*, 180–192.
[55] K. A. Youdim, M. Z. Qaiser, D. J. Begley, C. A. Rice-Evans, N. J. Abbott, *Free Radic Biol Med* **2004**, *36*, 592–604.
[56] S. S. Dahham, Y. M. Tabana, M. A. Iqbal, M. B. Ahamed, M. O. Ezzat, A. S. Majid, A. M. Majid, *Molecules* **2015**, *20*, 11808–11829.
[57] S. P. N. Bukke, C. Venkatesh, S. B. Rajanna, T. S. Saraswathi, P. K. Kusuma, N. Goruntla, N. Balasuramanyam, S. Munishamireddy, *Discover Applied Sciences* **2024**, *6*, 1–25.
[58] U. Bulbake, S. Doppalapudi, N. Kommineni, W. Khan, *Pharmaceutics* **2017**, *9*, 12.
[59] S. B. Carneiro, F. I. Costa Duarte, L. Heimfarth, J. D. Siqueira Quintans, L. J. Quintans-Júnior, V. F. da Veiga Júnior, A. A. Neves de Lima, *Int. J. Mol. Sci.* **2019**, *20*, https://doi.org/10.3390/IJMS20030642.
[60] M. Jaiswal, R. Dudhe, P. K. Sharma, *3 Biotech.* **2015**, *5*, 123–127.
[61] Y. Boulaamane, I. Touati, I. Qamar, I. Ahmad, H. Patel, A. Chandra, M. R. Britel, A. Maurady, *Chemistry Africa* **2024**, 1–23, https://doi.org/10.1007/S42250-024-01074-2/METRICS.
[62] Y. Boulaamane, I. M. Panadero, A. Hmadcha, C. A. Rey, S. Baammi, A. E. Allali, A. Maurady, Y. Smani, *mSystems* **2024**, *9*, e00324.
[63] Y. Boulaamane, K. Jangid, M. R. Britel, A. Maurady, *Mol. Divers.* **2023**, 1–17, https://doi.org/10.1007/S11030-023-10691-X/METRICS.
[64] M. S. Kondratyev, V. R. Rudnev, K. S. Nikolsky, D. V. Petrovsky, L. I. Kulikova, K. A. Malsagova, A. A. Stepanov, A. T. Kopylov, A. L. L, *Int. J. Mol. Sci.* **2022**, *23*, 16096.
[65] M. Thangavel, V. Chandramohan, H. S. Lalithamba, R. L. Jayaraj, P. Kumaradhas, M. Sivanandam, G. Hunday, R. Vijayakumar, R. Balakrishnan, D. Manimaran, N. Elangovan, *Sci. Rep.* **2020**, *10*, 1–10.
[66] T. Joshi, T. Joshi, P. Sharma, S. Chandra, V. Pande, *J. Biomol. Struct. Dyn.* **2021**, *39*, https://doi.org/10.1080/07391102.2020.1719200.
[67] O. Abchir, O. Daoui, S. Belaidi, M. Ouassaf, F. A. Qais, S. ElKhattabi, S. Belaaouad, S. Chtita, *J. Mol. Model.* **2022**, *28*, https://doi.org/10.1007/s00894-022-05097-9.
[68] A. Hidayatullah, W. E. Putra, Sustiprijatno, D. W., W. O. Salma, M. F. Heikal, *Trends in Sciences* **2023**, *20*, doi: 10.48048/tis.2023.4891.
[69] R. Shukla, H. Shukla, A. Sonkar, T. Pandey, T. Tripathi, *J. Biomol. Struct. Dyn.* **2018**, *36*, https://doi.org/10.1080/07391102.2017.1341337.

Manuscript received: July 22, 2024